Atmos. Meas. Tech., 11, 5389–5402, 2018
https://doi.org/10.5194/amt-11-5389-2018

Atmospheric Measurement Techniques
Open Access
EGU

The instrument constant of sky radiometers (POM-02) – Part 2: Solid view angle

Akihiro Uchiyama[1], **Tsuneo Matsunaga**[1], **and Akihiro Yamazaki**[2]

[1]Center for Global Environmental Research, National Institute for Environmental Studies, Tsukuba, Ibaraki 305-8506, Japan
[2]Meteorological Research Institute, Japan Meteorological Agency, Tsukuba, Ibaraki 305-0052, Japan

Correspondence: Uchiyama Akihiro (uchiyama.akihiro@nies.go.jp)

Received: 30 November 2017 – Discussion started: 11 January 2018
Revised: 1 June 2018 – Accepted: 11 July 2018 – Published: 26 September 2018

Abstract. Ground-based networks have been developed to determine the spatiotemporal distribution of aerosols using sky radiometers. In this study, errors related to the solid view angle (SVA) of sky radiometers, which are used by SKYNET, were investigated. The SVA is calculated using solar disk scan data, the measured radiances around the solar direction in $0.1 \times 0.1^\circ$ increments. These measurements include the scattered light from aerosol and air molecules, as well as the direct solar irradiance, causing errors in the SVA calculation. The influence of these errors was evaluated with simulations. From the results of these simulations if the aerosol optical depth (optical path length) is less than 0.5 (0.58) at 550 nm and the aerosol does not include large particles, such as desert dust particles, then its influence on the SVA calculation was less than 0.5 %. Problems with the software for the SVA calculation were also investigated. First, the data processing does not consider the change of airmass (solar zenith angle) during the solar disk scan measurement. In practice if a measurement is made in the period when the change in airmass is small, then the error is small. Second, before starting data processing, the minimum measured value is subtracted from the measured values, resulting in underestimation of the SVA by 1 % to 4 %. Thirdly, the values between 1.4 and 2.5° are not properly extrapolated, resulting in overestimation of the SVA by 0.6 % to 2.1 %. The second and third error sources partially cancel each other out, and the total error is an underestimation of 0.5 % to 1.9 % of the actual value. Furthermore, the annual trend in the SVA was examined. In both the visible and near-infrared regions (Si photodiode region) and in the shortwave-infrared region (InGaAs photodiode region), this trend cannot be seen in 4 and 8 years of data, respectively. The seasonal variation of the SVA was also examined, but no clear seasonal variation could be detected.

1 Introduction

Atmospheric aerosols are an important constituent of the atmosphere. Aerosols affect not only the global climate through the radiation budget both directly and indirectly (e.g., Ramanathan et al., 2001; Lohmann and Feichter, 2005) but also human health as one of the main components of air pollution.

Atmospheric aerosols have a large variability in time and space. To measure the spatiotemporal distribution of aerosols, ground-based observation networks such as AERONET (AErosol RObotic NETwork) (Holben et al., 1998) and SKYNET (Takamura et al., 2004) have been developed and extended, and remote sensing methods from space have been developed using the near-ultraviolet to shortwave-infrared wavelengths.

For ground-based observations, the solar direct irradiance and sky radiances are measured, and the aerosol characteristics are retrieved by analyzing these data. To improve the measurement accuracy, it is important to know the characteristics of the instrument and to be able to accurately calibrate it.

In SKYNET, radiometers POM-01 and POM-02 manufactured by Prede Co. Ltd., Japan are used. These radiometers are called "sky radiometers" and measure both the solar direct irradiance and sky radiances. The objectives in this study are to investigate the current status and issues with sky radiometers.

There are two constants that we must determine to be able to make accurate measurements. One is the calibration constant. The other is the solid view angle (SVA) of the radiometer. In Part 1 (Uchiyama et al., 2018), the temperature dependence of the sensor output was investigated and the calibration constants determined by the improved Langley method and normal Langley method were compared. An alternative method to determine the calibration constant for the 940 nm channel and the shortwave-infrared channels (1225, 1627, 2200 nm) was shown using on-site measurement data.

In Part 2, the problem related to the SVA of the sky radiometer is described. The SVA connects the sensor output to the sky radiance, which has units of energy/wavelength/sr. Overestimation (underestimation) in the SVA leads to underestimation (overestimation) of the single-scattering albedo (SSA). Therefore, it is necessary to accurately determine the SVA (Khatri et al., 2016; Hashimoto et al., 2012).

In Sect. 2, the accuracy of the current method for the SVA calculation is investigated based on simulations. Then, in Sect. 3, we describe the problem with the current SVA calculation program. This software is attached to the SKYRAD package (Nakajima et al., 1996), which is used to retrieve aerosol parameters from sky radiometer data. In Sect. 4, we also show the trend in the SVA and seasonal variation using the data obtained at MLO and JMA/MRI. In Sect. 5, the results and conclusions are presented.

2 Simulation study of SVA estimation error

The sensor output V when measuring the radiances from the sky with a sky radiometer can be written as follows:

$$V = \int_{\Delta} C(\lambda_0) f(\Omega) I(\Omega) \mathrm{d}\Omega \quad (1)$$
$$= C(\lambda_0) \overline{I} \Delta\Omega,$$

where C is the sensitivity, $I(\Omega)$ is the sky radiance in the direction of Ω, $f(\Omega)$ is the response function of the radiometer field of view,

$$\overline{I} = \int_{\Delta} f(\Omega) I(\Omega) \mathrm{d}\Omega / \Delta\Omega, \quad (2)$$

$$\Delta\Omega = \int_{\Delta} f(\Omega) \mathrm{d}\Omega, \quad (3)$$

and, for simplicity, the wavelength integration is omitted. Here, $\Delta\Omega$ is the SVA, which is related to the mean sky radiance in the direction of Ω, and errors in the SVA result in errors in the retrieved SSA. Therefore, the SVA is an important instrument parameter.

The SVA can be obtained by integrating the output of parallel light incident on the radiometer from all directions (see Appendix A). The SVA can also be obtained even if the light source has a finite size: the SVA can be obtained by integrating the output obtained while scanning the light source (see Appendix B).

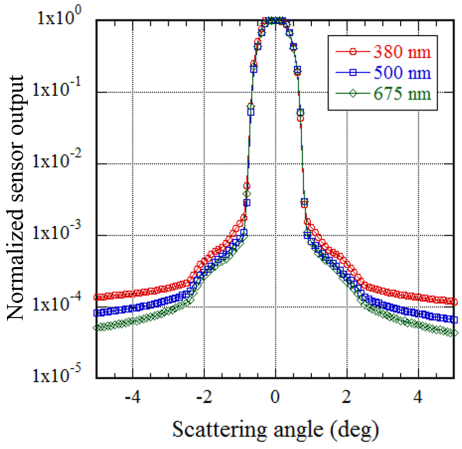

Figure 1. An example of measurement of the sun and the sky around the sun. The measurement was performed keeping the same azimuth angle as the solar azimuth angle. A positive (negative) value means a higher (lower) solar elevation, where the wavelengths are 380 nm (red), 500 nm (blue), and 675 nm (green). The values are normalized by the measured value at the zero scattering angle (direct solar irradiance).

To determine the SVA, a method using the measurement data around the sun was proposed by Nakajima et al. (1996). The radiances around the direction of the sun in $0.1 \times 0.1°$ increments are measured; this is called a "solar disk scan". Using these data, the SVA is calculated. Using similar gridded data, Torres et al. (2013) calculated the SVA of the Cimel-318 Sun-photometer and compared it with the values obtained by other methods.

An example of measurements of the radiance of the sun and around the sun is shown in Fig. 1. The measurements at POM-02 were performed vertically at intervals in the scattering angle of 0.1°, where the wavelengths are 380, 500, and 675 nm. Here, "vertically" means that the measurements were performed while keeping the azimuth angle the same as the solar azimuth angle. In Fig. 1, the values are normalized by the measured value at the zero scattering angle (the direct solar irradiance), where a positive (negative) value means a higher (lower) solar elevation. At any wavelength, the output of POM-02 changes greatly around the scattering angles of -2.5 and 2.5°. This means that the output of POM-02 is affected by the direct solar irradiance up to about ±2.5° from the sun direction.

The hood of POM-02 is designed so that the full field of view (FOV) is 1°. The size of the sun disk is about 0.5°. Therefore, the direct solar irradiance can enter the detector for angles up to about 0.75° from the sun's center. For ideal instruments, the output outside about 0.75° should be the output due to light scattered by air molecules and atmospheric

aerosols. However, Fig. 1 shows that the sensor output of POM-02 is affected by the direct solar irradiance for angles up to about ±2.5° from the sun's center.

The cause of the increase in the output between 0.75 and 2.5° is considered to be stray light. As the length of the hood and the size of the lens are finite, even if the angle from the sun center exceeds 0.75°, the direct solar light strikes the lens and results in "stray" light. This stray light reaches the detector and increases the output, and is smaller than the measurement of the direct sun by three orders of magnitude or more, but the integrated value has a magnitude that can affect the estimation of the SVA. Furthermore, when solar light is used as the light source, aerosols and air molecules exist between the light source and the instrument. Therefore, the scattered light from aerosols and air molecules is included in the measurement of the direct solar irradiance. The influence of this scattered light must also be considered.

As seen from Fig. 1, roughly speaking, the FOV of POM-02 consists of a core from 0 to 0.5° and a wing from 0.5 to 2.5°.

$$\begin{aligned}\Delta\Omega &= \Delta\Omega(\text{core}) + \Delta\Omega(\text{wing}) \\ &= \int_{\Delta\Omega(\text{core})} f(\Omega)\mathrm{d}\Omega + \int_{\Delta\Omega(\text{wing})} f(\Omega)\mathrm{d}\Omega\end{aligned} \tag{4}$$

Estimating the magnitudes of the two terms gives the following:

$$\begin{aligned}\Delta\Omega(\text{core}) &= \int_{\Delta\Omega(\text{core})} f(\Omega)\mathrm{d}\Omega \\ &\cong \int_{\Delta\Omega(\text{core})} 1\cdot\mathrm{d}\Omega \\ &= 2\pi(1-\cos(0.5^\circ)) \\ &= 2.39\times10^{-4},\end{aligned} \tag{5}$$

$$\begin{aligned}\Delta\Omega(\text{wing}) &= \int_{\Delta\Omega(\text{wing})} f(\Omega)\mathrm{d}\Omega \\ &\cong \int_{\Delta\Omega(\text{wing})} f_{\text{wing}}\mathrm{d}\Omega \\ &= 2\pi(\cos(0.5^\circ)-\cos(2.5^\circ))f_{\text{wing}} \\ &= 5.74\times10^{-3} f_{\text{wing}}.\end{aligned} \tag{6}$$

As seen from Fig. 1, $f_{\text{wing}} \approx 10^{-3}$. Therefore, the ratio of the terms is as follows:

$$\frac{\Delta\Omega(\text{wing})}{\Delta\Omega(\text{core})} \approx \frac{5.74\times10^{-3} f_{\text{wing}}}{2.39\times10^{-4}} = 2.4\times10^{-2}. \tag{7}$$

This means that neglecting the wing results in underestimation of the magnitude of the SVA by about 2 %. If $f_{\text{wing}} \approx 10^{-2}$, then the contribution of the wing to the SVA is about 20 %, and the instrument should be repaired. If $f_{\text{wing}} \approx 10^{-4}$, then the contribution is about 0.2 %, and the wing can be ignored. The magnitude of the sensor output between 0.75 and 2.5° depends on the internal structure of the skyradiometer and the optical constant of the material.

When the direction of the sun is measured, the sensor output $V(\Omega = 0)$ is as follows:

$$\begin{aligned}&V(\Omega=0) \\ &= C\left[\int_{\Delta} f(\Omega')I_0 g(\Omega')\mathrm{d}\Omega' + \int_{\Delta\Omega} I_{\text{sca}}(\Omega')f(\Omega')\mathrm{d}\Omega'\right] \\ &= v(0) + C\Delta\Omega\overline{I}_{\text{sca}}(0),\end{aligned} \tag{8}$$

where

$$v(0) = C\int_{\Delta} f(\Omega')I_0 g(\Omega')\mathrm{d}\Omega', \tag{9}$$

$$\overline{I}_{\text{sca}}(0) = \frac{1}{\Delta\Omega}\int_{\Delta\Omega} I_{\text{sca}}(\Omega')f(\Omega')\mathrm{d}\Omega', \tag{10}$$

and $I_0 g(\Omega')$ is the solar radiance distribution. The first term on the right-hand side of Eq. (8) is the contribution of the direct solar irradiance, and the second term is that of the scattered radiance.

When the direction of the sun is $\Omega = \Omega_0$, the sensor output $V(\Omega = \Omega_0)$ is as follows:

$$\begin{aligned}&V(\Omega=\Omega_0) \\ &= C\left[\int_{\Delta} f(\Omega_0+\Omega')I_0 g(\Omega')\mathrm{d}\Omega' + \int_{\Delta\Omega} I_{\text{sca}}(\Omega_0+\Omega')f(\Omega')\mathrm{d}\Omega'\right] \\ &= v(\Omega_0) + C\Delta\Omega\overline{I}_{\text{sca}}(\Omega_0),\end{aligned} \tag{11}$$

where the first term on the right-hand side is the contribution of the direct solar irradiance, and the second term is the scattered radiance. If Ω_0 is outside of the field of view, then the first term is zero and only the second term is needed.

Currently, based on the data of the solar disk scan measurement, the SVA is calculated by the following equation:

$$\Delta\Omega' = \int_{\Delta\Omega} \frac{v(\Omega) + \Delta\Omega C\overline{I}_{\text{sca}}(\Omega)}{v(0) + \Delta\Omega C\overline{I}_{\text{sca}}(0)}\mathrm{d}\Omega. \tag{12}$$

If there is no scattered radiance, then

$$\Delta\Omega' = \int_{\Delta\Omega} \frac{v(\Omega)}{v(0)}\mathrm{d}\Omega, \tag{13}$$

where $\Delta\Omega'$ is the SVA $\Delta\Omega$ (see Appendices A, B).

If the contribution of the scattered radiance is small, then $\Delta\Omega' \cong \Delta\Omega$. When the optical depth is large or the forward

scattering is dominant, the contribution of the scattered radiances increases.

We estimate the magnitude of each term of the integrand:

$$\frac{v(\Omega)+\Delta\Omega C\overline{I}_{\rm sca}(\Omega)}{v(0)+\Delta\Omega C\overline{I}_{\rm sca}(0)}=\frac{v(\Omega)+\Delta\Omega C\overline{I}_{\rm sca}(\Omega)}{v(0)(1+\Delta\Omega C\overline{I}_{\rm sca}(0)/v(0))}. \tag{14}$$

Usually, the solar disk scan measurement is performed only when the scattered light is much less than the direct solar irradiance:

$$\Delta\Omega C\overline{I}_{\rm sca}(0)/v(0)\ll 1.$$

The magnitude of this term has already been estimated from the influence of the scattered radiance in the field of view in the measurement of the sun-photometer; the estimation error of the optical depth due to the scattered radiance in the field of view (Zhao et al., 2012; Sinyuk et al., 2012).

Equation (14) can be approximated as follows:

$$\begin{aligned}&\frac{v(\Omega)+\Delta\Omega C\overline{I}_{\rm sca}(\Omega)}{v(0)+\Delta\Omega C\overline{I}_{\rm sca}(0)} \qquad (15)\\ &\cong\frac{v(\Omega)+\Delta\Omega C\overline{I}_{\rm sca}(\Omega)}{v(0)}\left(1-\frac{\Delta\Omega C\overline{I}_{\rm sca}(0)}{v(0)}\right)\\ &=\frac{v(\Omega)+\Delta\Omega C\overline{I}_{\rm sca}(\Omega)}{v(0)}(1-\varepsilon_3)\\ &=\frac{v(\Omega)}{v(0)}+\frac{\Delta\Omega C\overline{I}_{\rm sca}(\Omega)}{v(0)}-\frac{v(\Omega)}{v(0)}\varepsilon_3-\frac{\Delta\Omega C\overline{I}_{\rm sca}(\Omega)}{v(0)}\varepsilon_3,\end{aligned}$$

where

$$\varepsilon_3=\frac{\Delta\Omega C\overline{I}_{\rm sca}(0)}{v(0)}. \tag{16}$$

Therefore, Eq. (12) is as follows:

$$\begin{aligned}&\Delta\Omega' \qquad (17)\\ &=\int_{\Delta\Omega}\frac{v(\Omega)+\Delta\Omega C\overline{I}_{\rm sca}(\Omega)}{v(0)+\Delta\Omega C\overline{I}_{\rm sca}(0)}{\rm d}\Omega\\ &\cong\Delta\Omega+\Delta\Omega\int_{\Delta\Omega}\frac{C\overline{I}_{\rm sca}(\Omega)}{v(0)}{\rm d}\Omega-\Delta\Omega\varepsilon_3\\ &\quad-\Delta\Omega\int_{\Delta\Omega}\frac{C\overline{I}_{\rm sca}(\Omega)}{v(0)}{\rm d}\Omega\varepsilon_3\\ &=\Delta\Omega\left\{1+\int_{\Delta\Omega}\frac{C\overline{I}_{\rm sca}(\Omega)}{v(0)}{\rm d}\Omega-\varepsilon_3-\varepsilon_3\int_{\Delta\Omega}\frac{C\overline{I}_{\rm sca}(\Omega)}{v(0)}{\rm d}\Omega\right\}.\end{aligned}$$

As $v(0)=CF_0$, where F_0 is the solar irradiance and C is the proportional constant (sensitivity) (see Appendix B), the above Eq. (17) becomes

$$\begin{aligned}\Delta\Omega'&\cong\Delta\Omega\left\{1+\int_{\Delta\Omega}\frac{\overline{I}_{\rm sca}(\Omega)}{F_0}{\rm d}\Omega-\varepsilon_3-\varepsilon_3\int_{\Delta\Omega}\frac{\overline{I}_{\rm sca}(\Omega)}{F_0}{\rm d}\Omega\right\} \qquad (18)\\ &=\Delta\Omega\{1+\varepsilon_2-\varepsilon_3-\varepsilon_2\varepsilon_3\},\end{aligned}$$

in which

$$\varepsilon_2=\int_{\Delta\Omega}\frac{\overline{I}_{\rm sca}(\Omega)}{F_0}{\rm d}\Omega. \tag{19}$$

The fourth term is smaller than the second and third terms and it can be ignored. Then, comparing the second and third terms in the curly brackets,

$$\begin{aligned}\varepsilon_2&=\int_{\Delta\Omega}\frac{\overline{I}_{\rm sca}(\Omega)}{F_0}{\rm d}\Omega \qquad (20)\\ &=\int_{\Delta\Omega}\left\{\frac{1}{F_0}\cdot\frac{1}{\Delta\Omega}\int_{\Delta\Omega}I_{\rm sca}(\Omega+\Omega')f(\Omega'){\rm d}\Omega'\right\}{\rm d}\Omega,\\ \varepsilon_3&=\frac{\Delta\Omega}{F_0}\cdot\frac{1}{\Delta\Omega}\int_{\Delta\Omega}I_{\rm sca}(0+\Omega')f(\Omega'){\rm d}\Omega' \qquad (21)\\ &=\frac{\Delta\Omega\overline{I}_{\rm sca}(\Omega=0)}{F_0},\end{aligned}$$

where ε_2 is the integral of the mean scattered light $\overline{I}_{\rm sca}(\Omega)$ in the region of $f(\Omega)>0$, and ε_3 is the integral of scattered light in the FOV when facing toward the sun.

The $f(\Omega)$ of the POM-02 consists of the core from 0.0 to 0.5°, which takes large values, and the wing from 0.5 to 2.5° which takes small values. Therefore, the integral can be written as follows:

$$\begin{aligned}\varepsilon_2&=\int_{\Delta\Omega}\frac{\overline{I}_{\rm sca}(\Omega)}{F_0}{\rm d}\Omega \qquad (22)\\ &=\int_{\Delta\Omega({\rm core})}\frac{\overline{I}_{\rm sca}(\Omega)}{F_0}{\rm d}\Omega+\int_{\Delta\Omega({\rm wing})}\frac{\overline{I}_{\rm sca}(\Omega)}{F_0}{\rm d}\Omega,\end{aligned}$$

As $\overline{I}_{\rm sca}(\Omega)\approx\overline{I}_{\rm sca}(\Omega=0)$ in the core, $\int_{\Delta\Omega({\rm wing})}f(\Omega){\rm d}\Omega\ll 1$, and $\int_{\Delta\Omega({\rm core})}{\rm d}\Omega\cong\Delta\Omega$, the first term of the integral ε_2 is as follows:

$$\int_{\Delta\Omega({\rm core})}\frac{\overline{I}_{\rm sca}(\Omega)}{F_0}{\rm d}\Omega\cong\frac{\overline{I}_{\rm sca}(\Omega=0)}{F_0}\Delta\Omega. \tag{23}$$

This means that the integral of the core in the integral ε_2 has the same magnitude as ε_3 and the two terms offset each other,

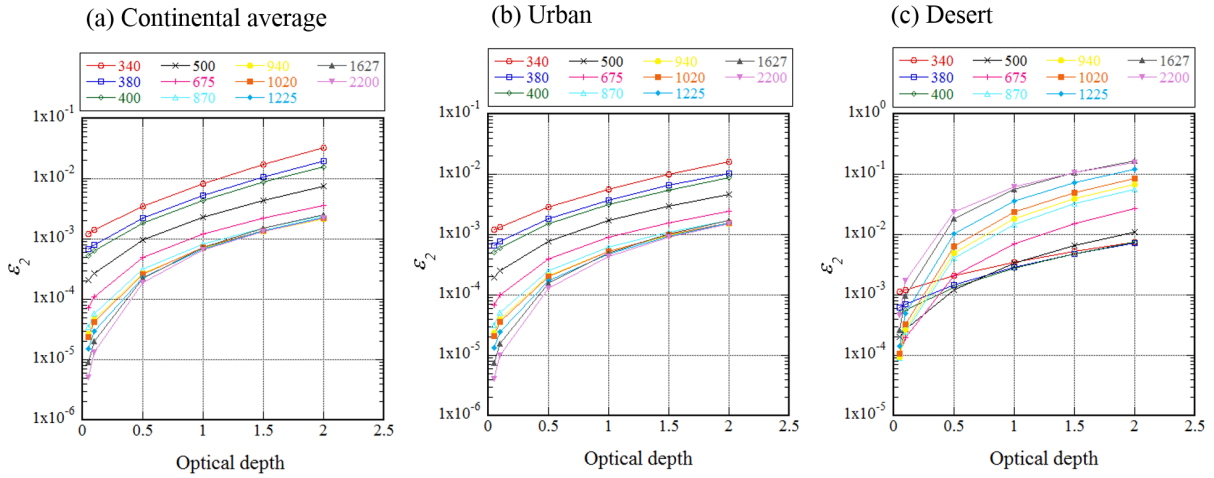

Figure 2. Estimation of the error ε_2 in the calculation of the SVA. Aerosol models are the OPAC continental average, urban, and desert. The aerosol optical depth thickness is that at a wavelength of 550 nm and the solar zenith angle is 30°.

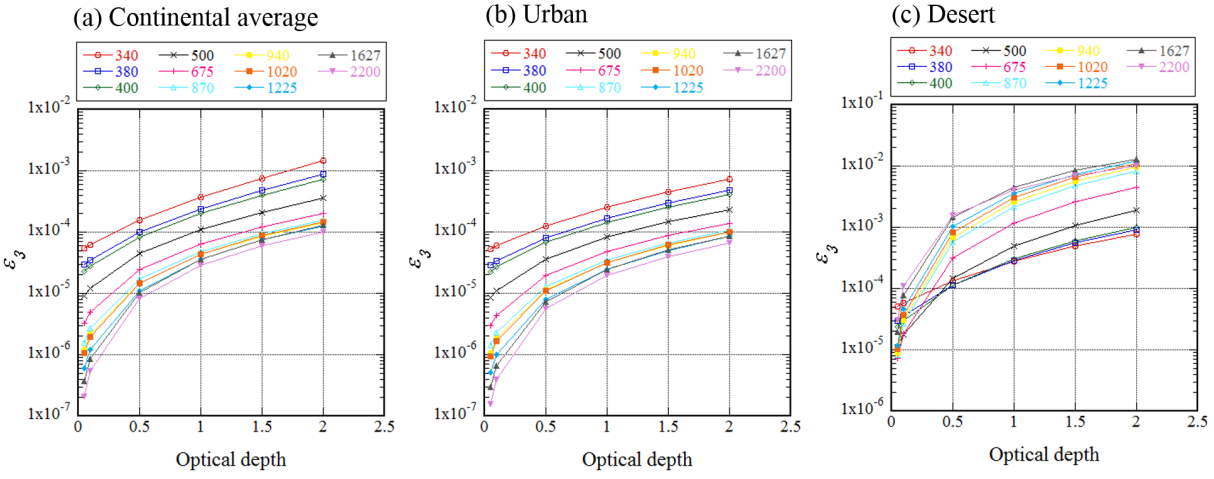

Figure 3. Same as Fig. 2 but for error ε_3.

whereas the integral of the wing remains. The area of the integral of the wing is larger than that of the core. Even if the integral of scattered light in the FOV is small compared to the solar direct irradiance, the integral of the wing becomes large and introduces errors in the SVA estimation. That is, even if the measurement value of scattered light is smaller than the direct sun measurement, $\overline{I}_{\mathrm{sca}}(\Omega)\Delta\Omega/F_0 \approx 10^{-3}$, the integral of the wing becomes large:

$$\int_{\Delta\Omega(\mathrm{wing})} \frac{\overline{I}_{\mathrm{sca}}(\Omega)}{F_0} \mathrm{d}\Omega \approx \frac{\Delta\Omega(\mathrm{wing})}{\Delta\Omega} \times 10^{-3} \approx \frac{\Delta\Omega(\mathrm{wing})}{\Delta\Omega(\mathrm{core})} \times 10^{-3} = 2.4 \times 10^{-2}. \quad (24)$$

In this case, the magnitude of the error is about 2 %.

Figures 2 and 3 show the values of ε_2 and ε_3 when the aerosol optical depth at 550 nm is changed. Here, the solar zenith angle is 30° and the aerosol models are the OPAC continental average, urban, and desert types (Hess et al., 1998). The simulation calculations of the scattered sky radiances were performed using the subroutine in the SKYRAD package. The Ångström exponents of the continental average in the shorter (350 to 500 nm) and longer (500 to 800 nm) wavelength regions are 1.11 and 1.42, respectively. Those of the urban areas are 1.14 and 1.43, respectively, and those of the desert are 0.20 and 0.17, respectively.

When comparing ε_2 and ε_3, the signs are opposite and partially cancel out. However, ε_3 is one order of magnitude smaller than ε_2, and thus ε_2 contributes to the error in the calculation of the SVA. In the continental average and urban models if the aerosol optical depth (optical

path length = optical depth × airmass) at 550 nm is less than $0.5(0.50/\cos(30°) = 0.58)$, then the second term ε_2 is less than 0.5 %, and if the aerosol optical depth at 550 nm is less than 1, then the second term ε_2 is less than 1 %. In the desert model, which includes large particles, the second term is less than 1 % for shorter wavelengths, where desert particles have a higher absorption than in the longer wavelength regions. However, even if the aerosol optical depth at 550 nm is less than 0.5, the second term is larger than 1 % for some wavelengths.

From these simulations if the scattered light can be removed from the SVA calculation, then an improvement in the accuracy of the calculations can be expected. However, as the intensity of the scattered light depends on aerosol characteristics, it is difficult to estimate the intensity of the scattered light from the measurements. Furthermore, close to the sun the value of scattered light cannot be measured due to the direct sunlight. In POM-01 and POM-02, scattered light can only be measured without being affected by direct sunlight at scattering angles of more than 3°.

The SVA was calculated by subtracting the measurements for a scattering angle of 3° and the accuracy of the estimation was examined. Although not shown in detail, for the continental average and urban models, even if the aerosol optical depth (optical path length) is 2 (2.3) at 550 nm, the error in the SVA estimation was less than 0.5 %. This indicates that if the measured value of scattered light can be subtracted, the estimation accuracy of the SVA can be greatly improved.

From these results, when we determine the SVA by using the data from the solar disk scan measurement if the aerosol optical depth (optical path length) is less than 0.5 (0.58) and the aerosol does not include large particles such as desert dust particles, the effect of the scattered radiances on the SVA calculation is less than 0.5 %, and $\Delta\Omega$ is well approximated by $\Delta\Omega'$. Furthermore if the measured value of the scattered light can be subtracted, the estimation accuracy of SVA can be greatly improved.

3 SVA calculation with the SKYRAD package

The software in the SKYRAD package (Nakajima et al., 1996) is often used for SVA calculation from the data of the solar disk scan measurement. However, the authors noticed that there are problems in this program, and this section investigates these problems in detail. In Appendix C, a flowchart is shown illustrating the SVA calculation procedure in the SKYRAD package.

In the measurement of the solar disk scan, a range of ±1° in the zenith angle direction and ±1° in the azimuth direction relative to the sun in increments of 0.1° is used, which produces a 21 × 21 grid with an angular resolution of 0.1°. Therefore, the data are taken from the sun for scattering angles of up to about $1.4(= (1°) \times \sqrt{2})°$. As shown in Fig. 1, the influence of the direct solar irradiance as a light source extends to about 2.5°. To take this into consideration, the integration is performed by extrapolation for angles larger than 1.4°.

The following three problems exist in the SKYRAD package for calculating the SVA.

First, the data processing does not consider changes in the airmass (solar zenith angle) during the solar disk scan measurement. However, in practice, if the solar disk scan measurement is conducted when the airmass change (solar zenith angle) is small, then the resulting error is also small. Also, this is not usually a problem unless the measurement is conducted over an extended period of time.

Second, before starting the data processing, the minimum measured value is subtracted from the measured values. As a result, the measurements of the scattering angle between 1 and 1.4° are greatly affected. By integrating the measured value minus the minimum, the SVA is always underestimated, but the solution to this problem is not straightforward.

Thirdly, the values between 1.4 and 2.5° are not properly extrapolated. Frequently, the extrapolated value does not decrease monotonically. In some cases, this partially cancels out the underestimation of the integral.

In Fig. 4, an example of the integrand for the SVA calculation is shown. In the blue curve with open squares, the minimum value is subtracted. This curve is then integrated by the current SKYRAD program. As the minimum value is subtracted, the difference is noticeable at scattering angles greater than 1°. In this case, the extrapolated value from 1.4 to 2.5° is almost constant. In many cases, nearly constant values were extrapolated as in this example. In some cases, the extrapolated values increased. In the red curve with open circles, the minimum value is not subtracted. The values between 1.4 and 2.5° were extrapolated using the data from 1.0 to 1.4°. Considering Fig. 1, the decreasing trend is more realistic. Furthermore, Manago et al. (2016) showed, using lamp-based measurements at the ground level, that the FOV monotonically decreases to around 2.5° and then sharply decreases as the scattering angle increases.

To investigate the differences in the calculation methods, several calculations were performed.

The following steps in the calculations were varied:

1. whether the minimum value was subtracted;
2. whether the change in airmass was considered;
3. the method for the extrapolation in the range from 1.4 to 2.5°;
4. whether the horizontal cross-section of the FOV is assumed to be a circle or an ellipse (the current SKYRAD package method uses an ellipse);
5. the method for determining the ellipse's parameters.

Data taken at MLO in October and November in 2015 were used in this study.

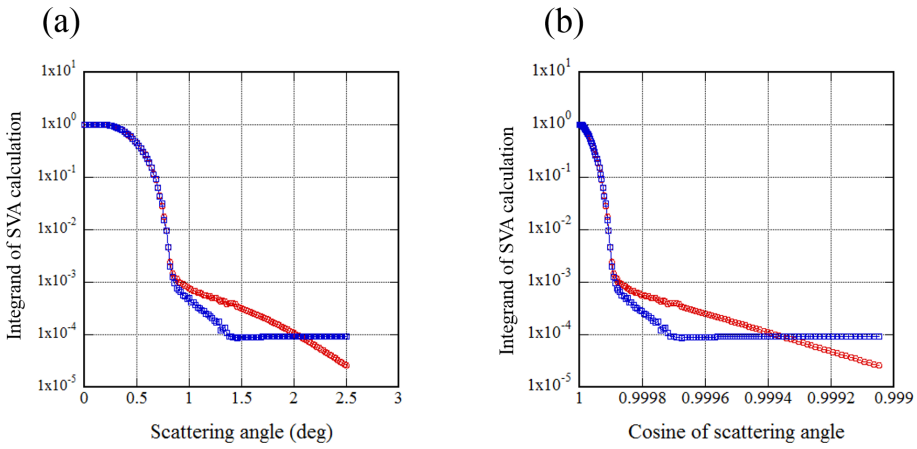

Figure 4. Example of the integrand of the SVA calculation. The blue line with open squares is for the case that the minimum value is subtracted, and the red line is for the case that the values between 1.4 and 2.5° are extrapolated using the data from 1.0 to 1.4°.

Table 1. Settings of the SVA calculation.

	Subtract minimum value	Consideration of airmass change	Extrapolation method	FOV shape
Case 1	yes	no	current	elliptic
Case 2	no	no	current	elliptic
Case 3	no	yes	current	elliptic
Case 4	no	yes	new	elliptic
Case 5	no	yes	current	circular
Case 6	no	yes	new	elliptic

Case 1 is the method implemented in the current SKYRAD package. In Case 5, "circular" means that the FOV is axisymmetric. The elliptic shape parameters in Case 6 are calculated by a different method from the SKYRAD package.

The solar disk scan measurement was made between 10:00 and 13:00 local time (LT) at MLO. The optical depth at wavelengths of 500 and 340 nm were at most 0.1 and 0.5, respectively. Therefore, the influence of the scattered light on the SVA calculation is small.

The SAV was calculated for the six cases shown in Table 1, including Case 1, which is the current method used by the SKYRAD package. In Cases 4 and 6, the values in the range 1.4 to 2.5° were extrapolated as a linear function of the cosine of the scattering angle. This linear function was determined by the least squares method using the data with a scattering angle of more than 1°. In Cases 3, 4, 5, and 6, assuming that the aerosol optical depth has not changed, the solar direct irradiance changes due to the change of the airmass during the measurement. The elliptic parameters in Case 6 were determined by assuming that the shape of the FOV is a 2-dimensional Gaussian distribution. The results of the comparison are summarized in Table 2.

The difference between Case 1 and Case 2 is whether or not the minimum value was subtracted. Case 1, in which the minimum value was subtracted, results in an underestimation of about 1 % to 4 %.

The standard deviation in the region of shorter wavelengths in Case 1 is smaller than for the other cases. One of the causes of the variation of the calculated SVA is the variation of the wing of the FOV. In the region of shorter wavelengths, generally, the optical depth is thicker than the longer wavelength region, and the scattered light increases in the shorter wavelength region. When the minimum value is subtracted from the measurement value, the value of the wing portion decreases greatly in the shorter wavelength region, and the contribution to the SVA integration also decreases greatly in the short wavelength region. As a result, the variance of the calculated SVA becomes small. However, there is no justification for subtracting the minimum value.

The difference between Case 2 and Case 3 is whether the change in airmass was considered or not. The solar disk scan measurement was made between 10:00 and 13:00 LT at MLO. Therefore, the change in the air mass is less than 0.01, and there was hardly any influence from the change in airmass.

The difference between Case 3 and Case 4 is the method of extrapolation used in the range from 1.4 to 2.5°. In the

Table 2. Influence of the different calculation settings. **(a)** Calculated SVA. The data taken at MLO in October and November 2015 are used. **(b)** Comparison of calculated SVA.

(a) WLN (nm)		340	380	400	500	675	870	940	1020	1225	1627	2200
Case_1 (C1)	SVA ($\times10^{-4}$)	2.4495	2.4643	2.4472	2.4366	2.4530	2.4404	2.4554	2.4567	2.0086	2.0152	2.0692
	SD ($\times10^{-4}$)	0.0379	0.0407	0.0403	0.0388	0.0374	0.0277	0.0296	0.0241	0.0287	0.0241	0.0214
	SD / SVA	0.0155	0.0165	0.0165	0.0159	0.0153	0.0113	0.0121	0.0098	0.0143	0.0120	0.0103
Case_2 (C2)	SVA ($\times10^{-4}$)	2.5014	2.5186	2.5036	2.4764	2.4782	2.4995	2.5322	2.5564	2.0586	2.0737	2.1328
	SD ($\times10^{-4}$)	0.1151	0.1116	0.1144	0.0838	0.0579	0.0346	0.0314	0.0257	0.0294	0.0260	0.0233
	SD / SVA	0.0460	0.0443	0.0457	0.0338	0.0234	0.0138	0.0124	0.0101	0.0143	0.0125	0.0109
Case_3 (C3)	SVA ($\times10^{-4}$)	2.5015	2.5184	2.5035	2.4765	2.4783	2.4993	2.5320	2.5565	2.0586	2.0737	2.1327
	SD ($\times10^{-4}$)	0.1151	0.1115	0.1144	0.0838	0.0580	0.0344	0.0315	0.0258	0.0295	0.0260	0.0233
	SD / SVA	0.0460	0.0443	0.0457	0.0338	0.0234	0.0138	0.0124	0.0101	0.0143	0.0125	0.0109
Case_4 (C4)	SVA ($\times10^{-4}$)	2.4693	2.4899	2.4698	2.4534	2.4641	2.4691	2.4923	2.5023	2.0346	2.0440	2.1005
	SD ($\times10^{-4}$)	0.0668	0.0804	0.0698	0.0580	0.0459	0.0304	0.0302	0.0259	0.0301	0.0259	0.0227
	SD / SVA	0.0271	0.0323	0.0283	0.0236	0.0186	0.0123	0.0121	0.0104	0.0148	0.0127	0.0108
Case_5 (C5)	SVA ($\times10^{-4}$)	2.5027	2.5199	2.5032	2.4777	2.4783	2.5010	2.5329	2.5565	2.0596	2.0750	2.1336
	SD ($\times10^{-4}$)	0.1155	0.1123	0.1141	0.0831	0.0583	0.0346	0.0312	0.0262	0.0298	0.0261	0.0236
	SD / SVA	0.0461	0.0446	0.0456	0.0335	0.0235	0.0138	0.0123	0.0102	0.0145	0.0126	0.0111
Case_6 (C6)	SVA ($\times10^{-4}$)	2.4694	2.5042	2.4698	2.4535	2.4637	2.4698	2.4921	2.5028	2.0349	2.0449	2.1014
	SD ($\times10^{-4}$)	0.0669	0.1249	0.0701	0.0576	0.0463	0.0297	0.0305	0.0264	0.0312	0.0258	0.0225
	SD / SVA	0.0271	0.0499	0.0284	0.0235	0.0188	0.0120	0.0122	0.0106	0.0153	0.0126	0.0107
No. of data		19	19	17	20	17	18	17	17	20	20	17

(b) WLN (nm)	340	380	400	500	675	870	940	1020	1225	1627	2200	
C2/C1-1	0.0212	0.0220	0.0230	0.0163	0.0103	0.0242	0.0313	0.0406	0.0249	0.0290	0.0307	min. value subtraction
C3/C2-1	0.0000	−0.0001	0.0000	0.0000	0.0000	−0.0001	−0.0001	0.0000	0.0000	0.0000	0.0000	airmass change
C4/C3-1	−0.0129	−0.0113	−0.0135	−0.0093	−0.0057	−0.0121	−0.0157	−0.0212	−0.0117	−0.0143	−0.0151	different extrapolation
C4/C1-1	0.0081	0.0104	0.0092	0.0069	0.0045	0.0118	0.0150	0.0186	0.0129	0.0143	0.0151	min. value subtraction, different extrapolation
C5/C3-1	0.0005	0.0006	−0.0001	0.0005	0.0000	0.0007	0.0004	0.0000	0.0005	0.0006	0.0004	circular or elliptic shape
C6/C4-1	0.0000	0.0057	0.0000	0.0000	−0.0002	0.0003	−0.0001	0.0002	0.0001	0.0004	0.0004	different elliptic parameters

current SKYRAD package, the SVA was overestimated by 0.6 % to 2.1 %.

As there was hardly any influence from the change in airmass, in Case 1 and Case 4 the underestimation caused by the subtraction of the minimum value and the overestimation caused by the poor extrapolation partially cancel each other out, and the current SKYRAD package method underestimates the SVA by 0.5 % to 1.9 %.

The difference between Case 3 and Case 5 is whether the horizontal cross-section of the FOV is assumed to be a circle or an ellipse. The difference between them was less than 0.1 %. This indicates that POM-02 was well tuned when it was shipped from the manufacturer.

In Case 6, a different method for determining elliptic parameters from the current SKYRAD package was used. Therefore, the difference between Case 4 and Case 6 is the difference between the methods used to determine the elliptic parameters. There was almost no difference between the current method and the new method. The method used to determine the elliptic parameters thus has little effect on the SVA estimation.

4 Annual trend and seasonal variation of SVA

Broadly speaking, the SVA is determined by the size of the pinhole and the focal length of the lens. There is a possibility that these parameters may change with degradation and the inside temperature. Therefore, the annual trend and seasonal variation of the SVA are examined.

Figures 5 and 6 show the SVAs in the visible and near-infrared region (Si photodiode) and in the shortwave-infrared region (InGaAs photodiode) for 2008 and 2016, respectively. The observation for the calibration at MLO was performed over about a month in October and November each year. The lens in the visible region was replaced before the observation in 2013.

In Fig. 5a, time series of the SVA in channels 1 to 8 (from 340 to 1020 nm) are shown for the SVA calculated by the corrected method in this study. In Fig. 5b, the SVA in channel 4 (500 nm) calculated by both the corrected and the current SKYRAD package methods are shown for comparison. As stated in the above section, the SVA calculated by the current method is lower than that calculated by the corrected one except for 2008. As the lens in the visible and near-infrared region was replaced before the calibration observation in 2013, it is difficult to investigate the annual trend of the SVA. Ad-

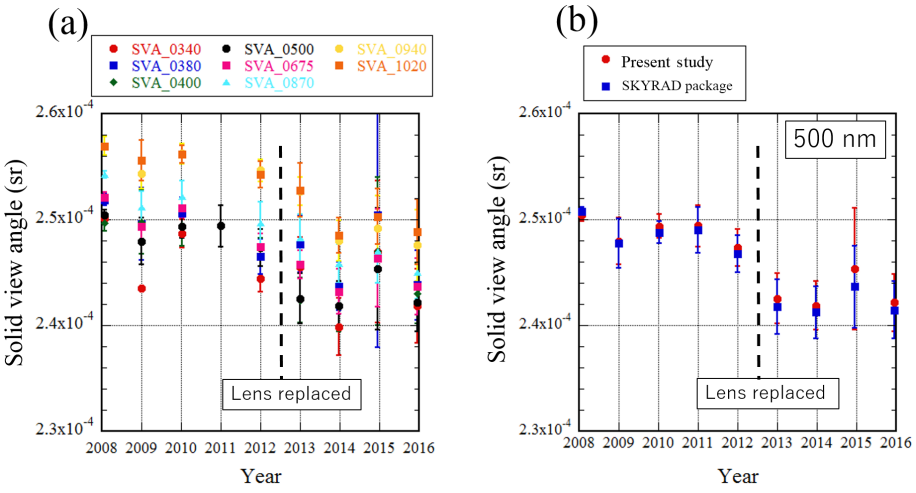

Figure 5. SVAs in the visible and near-infrared region (Si photodiode) from 2008 to 2016. The data were taken at MLO over a month in October and November every year. **(a)** SVA calculated by the corrected method in this study, **(b)** SVA at a wavelength of 500 nm calculated by both the corrected and the current SKYRAD package methods.

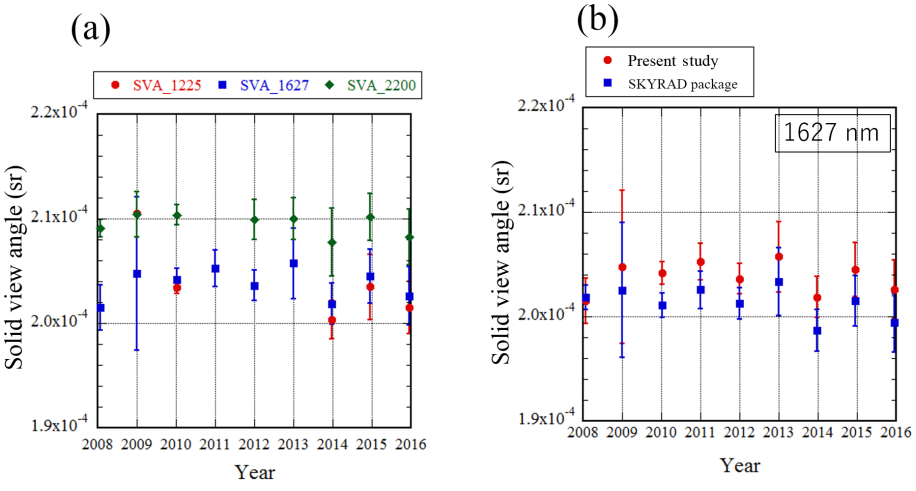

Figure 6. Same as Fig. 5 but for the shortwave-infrared region (InGaAs photodiode). The wavelength in **(b)** is 1627 nm.

ditionally, from this figure, the uncertainty of the SVA (the ratio of standard deviation/mean) is estimated at about 1 % except in 2015.

From 2008 to 2012, the value of the SVA seems to be decreasing. The value of the SVA in 2008 is larger than in other years. The mean values of the SVA are within ±0.5 % except in 2008. From 2013 to 2016, the mean values of the SVA are within ±1 %. The annual variation of the SVA is less than or equal to the uncertainty of the SVA. From these results, the annual trend in the SVA cannot be seen in only 4 years of data, and even if there is a trend, it is smaller than the measurement uncertainty.

Figure 6a is the same as Fig. 5a except for channels 9 to 11 (1225, 1627, 2200 nm) and Fig. 6b is the same as Fig. 5b except for channel 10 (1627 nm). In these channels, the SVA calculated by the current method is also lower than that calculated by the corrected one except in 2008.

The determination uncertainty of the SVA is also estimated as about 1 %. The lens in the shortwave-infrared region was not replaced in the period from 2008 to 2016. The trend in the SVA cannot be seen in 8 years of data either. The values of the SVA in this period are within ±1 %, which is the determination uncertainty of the SVA. From these results, the annual trend of the SVA in the shortwave-infrared channels cannot be seen in 8 years of data, and even if there is a trend, it is smaller than the measurement uncertainty.

Figure 7 shows the SVAs of POM-02 (Tsukuba) in the 500 and 1627 nm channels in the period from January 2014 to December 2016. All data are plotted and the data are scattered about ±1.5 % and ±2 % (the ratio of standard deviation/mean), though the values in 2014 are a bit low. There is

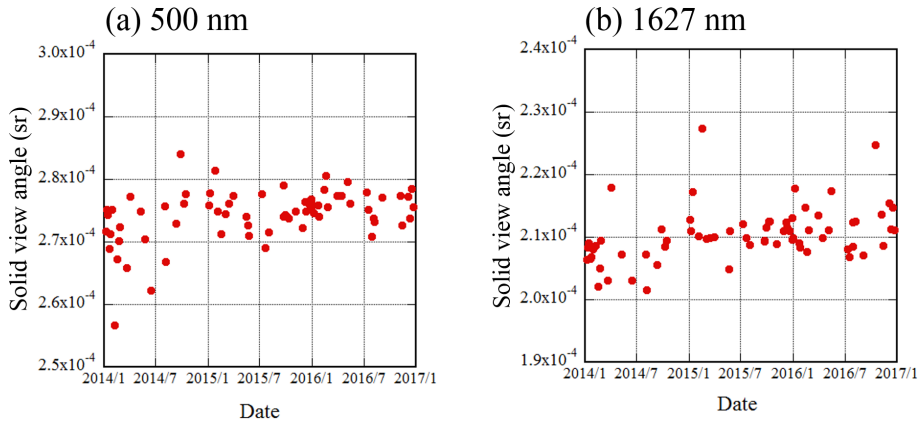

Figure 7. Time series of the SVA at POM-02 (Tsukuba) from January 2014 to December 2016. **(a)** 500 nm, the mean and standard deviation are 2.743×10^{-4} and 4.2×10^{-6}, respectively. **(b)** 1627 nm, the mean and standard deviation are 2.104×10^{-4} and 4.4×10^{-6}, respectively.

a large amount of data in the winter, because there are many fine days in the winter in Tsukuba. There are little data from spring to autumn and the data in the summer are scattered. As the estimated SVA is scattered, it is not possible to draw a clear conclusion, but as can be seen from Fig. 7, the seasonal variation exceeding ± 2 % cannot be confirmed in either channel. This also indicates that the temperature dependence of the SVA in both detector regions cannot be seen. As the data are taken over a short period of 3 years, no annual trend in the SVA can be detected.

5 Summary and conclusion

Atmospheric aerosols are an important constituent of the atmosphere. Measurement networks covering an extensive area from ground and space have been developed. SKYNET is a ground-based monitoring system using sky radiometers POM-01 and POM-02 (Prede Co. Ltd., Japan). To improve the measurement accuracy, it is important to know the characteristics of the instruments and calibrate them. There are two constants that we must determine to make accurate measurements. One is the calibration constant, and the other is the SVA of the radiometer.

In Part 1, problems related to the estimation of the calibration constant were investigated, and in Part 2, problems related to the determination of the SVA of the sky radiometer were described.

In this study, the data from two sky radiometers POM-02 of the JMA/MRI were analyzed. One of the sky radiometers was used as a calibration reference, and the other was used for the continuous measurement at the Tsukuba MRI observation site.

The FOV of POM-02 consists of a core from 0 to 0.5° and a wing from 0.5 to 2.5°. The wing is about 3 orders of magnitude smaller than the core, but the wing contributes about 2 % to the SVA.

A method for determining the SVA using the sun as a light source was proposed by Nakajima et al. (1996). In this method, the radiance around the direction of the sun in $0.1 \times 0.1°$ increments is measured. These measurements include the scattered light from aerosols and air molecules as well as the direct solar irradiance. These scattered radiances cause errors in the SVA calculation.

The influence of the scattered light was evaluated by simulations. As a result if the aerosol optical depth (optical path length) is less than 0.5 (0.58) at a wavelength of 550 nm and the aerosol does not include large particles such as desert dust particles, then the effect of the scattered radiances on the SVA calculation is less than 0.5 %. Furthermore if the measurements of the scattered light can be taken into account, the estimation accuracy of the SVA can be greatly improved.

The SKYRAD package for determining the SVA from the solar disk scan measurements has several problems. The problems do not result in major errors in the estimation of the SVA, but can cause a systematic underestimation.

First, the data processing does not consider the change in the airmass (solar zenith angle) during the solar disk scan measurement. In practice if the measurements are taken over a period when the change in airmass is small, then there is almost no problem. Second, before beginning the data processing, the minimum value is subtracted from each measured value. This results in an underestimation of the SVA by 1 % to 4 %. Thirdly, the values between 1.4 and 2.5° are not properly extrapolated. This overestimates the SVA value by 0.6 % to 2.1 %. As the second and third errors partially cancel each other out if the current software is used, the overall error will be an underestimation of 0.5 % to 1.9 %.

The annual trend in the SVA was examined using the data taken at MLO. As the optical depth at a wavelength of 500 nm is 0.1 at most at MLO, the influence of the scattered light is small. The uncertainty of the SVA was estimated as about 1 %. In the visible and near-infrared region, the annual trend in the SVA could not be seen in only 4 years of data

from 2009 to 2012 and 2013 to 2016, and it was smaller than the measurement accuracy. In the shortwave-infrared region, the annual trend of the SVA could not be seen in 8 years data from 2008 to 2016, and it was smaller than the measurement uncertainty.

The seasonal variation of the SVA was examined using the data taken at Tsukuba from January 2014 to December 2016. As the time series of the determined SVA was scattered over a range of $\pm 2\,\%$, it is not possible to draw a clear conclusion, but seasonal variation exceeding $\pm 2\,\%$ could not be confirmed. Furthermore, as the temporal range of the data was short, no annual trend could be detected.

According to the method based on the current measurement data, the uncertainty is $1\,\%$ at high-altitude mountain sites such as MLO and $1.5\,\%$ to $2\,\%$ at low-altitude sites such as Tsukuba. The cause of the error may be an increase in the scattered light in the optically thick case, a variation in the solar direct irradiance due to a change in the aerosol concentration during the solar disk scan measurement, and an error in the pointing direction of the FOV. In the future, we will eliminate scattered light and use measurements of the aerosol optical depth from other instruments during the solar disk scan measurement. We will also develop methods for measuring the SVA on the ground or in a laboratory.

Data availability. Data used in this study are available from the corresponding author.

Appendix A

Let $f(\Omega)$ be the response function of the FOV, where Ω indicates the direction, and when $\Omega = 0$, $f(\Omega = 0) = 1$.

The SVA is then as follows:

$$\Delta\Omega = \int_{\Delta} f(\Omega)\mathrm{d}\Omega. \tag{A1}$$

Suppose parallel light enters from $\Omega = \Omega_0$.

$$\begin{aligned} &V(\Omega = \Omega_0) \\ &= C\int_{\Delta} f(\Omega)\delta(\Omega - \Omega_0)F_0\mathrm{d}\Omega \\ &= Cf(\Omega = \Omega_0)F_0 \end{aligned} \tag{A2}$$

Here, F_0 is the input irradiance, and C is the proportional constant (sensitivity).

Therefore,

$$f(\Omega_0) = \frac{V(\Omega_0)}{CF_0}. \tag{A3}$$

As $f(0) = 1$, then $V(0) = CF_0$.

Therefore,

$$\begin{aligned} \Delta\Omega &= \int_{\Delta} f(\Omega)\mathrm{d}\Omega \\ &= \int_{\Delta} \frac{V(\Omega_0)}{CF_0}\mathrm{d}\Omega_0 \\ &= \int_{\Delta} \frac{V(\Omega_0)}{V(0)}\mathrm{d}\Omega_0. \end{aligned} \tag{A4}$$

When the parallel light is incident, the SVA of the radiometer can be obtained by integrating the output in an arbitrary direction normalized by the output in the direction of $\Omega = 0$.

Appendix B

Here, we consider the case that the light source has a finite size, for example, when the sun is used as a light source.

Let the radiance distribution of the light source be $I(\Omega) = I_0 g(\Omega)$.

The integrated energy of the light source F_0 is as follows:

$$F_0 = \int_{\Delta} g(\Omega) I_0 \mathrm{d}\Omega, \tag{B1}$$

where Δ is the extent of the light source.

Considering the sun as a light source, let Δ be smaller than $\Delta\Omega$. Also, when the sun is a light source, F_0 is the solar irradiance.

Let C be the sensitivity of the detector, where C is the proportional constant of the sensor output and input energy.

The light source is in the direction of $\Omega = 0$ and we measure the radiance from it as

$$v(0) = C\int_{\Delta} f(0 + \Omega')g(\Omega')I_0\mathrm{d}\Omega', \tag{B2}$$

where $v(0)$ is the sensor output.

If $f(\Omega)$ is constant within the range of Δ (POM-02 satisfies this condition), then this equation can be rewritten as follows:

$$\begin{aligned} v(0) &= CI_0\int_{\Delta} f(\Omega')g(\Omega')\mathrm{d}\Omega' \\ &= CI_0 f(0)\int_{\Delta} g(\Omega')\mathrm{d}\Omega' \\ &= Cf(0)F_0 \\ &= CF_0. \end{aligned} \tag{B3}$$

Next, the light source is in the direction of $\Omega = \Omega_0$:

$$v(\Omega_0) = CI_0\int_{\Delta} f(\Omega_0 + \Omega')g(\Omega')\mathrm{d}\Omega', \tag{B4}$$

where $v(\Omega_0)$ is the sensor output.

Then, both sides of the equation are integrated within the SVA $\Delta\Omega$:

$$\begin{aligned} &\int_{\Delta\Omega} v(\Omega_0)\mathrm{d}\Omega_0 \\ &= \int_{\Delta\Omega}\left(CI_0\int_{\Delta} f(\Omega_0 + \Omega')g(\Omega')\mathrm{d}\Omega'\right)\mathrm{d}\Omega_0. \end{aligned} \tag{B5}$$

By changing the order of integration on the right, the following equation can be obtained:

$$\begin{aligned} \int_{\Delta\Omega} v(\Omega_0)\mathrm{d}\Omega_0 &= CI_0\int_{\Delta}\left(g(\Omega')\int_{\Delta\Omega} f(\Omega_0 + \Omega')\mathrm{d}\Omega_0\right)\mathrm{d}\Omega' \\ &= CI_0\int_{\Delta} g(\Omega')\mathrm{d}\Omega' \cdot \Delta\Omega \\ &= CF_0\Delta\Omega. \end{aligned} \tag{B6}$$

Therefore, from Eqs. (B3) and (B6),

$$\begin{aligned} \Delta\Omega &= \frac{1}{CF_0}\int_{\Delta\Omega} v(\Omega_0)\mathrm{d}\Omega_0, \\ &= \int_{\Delta\Omega} \frac{v(\Omega_0)}{v(0)}\mathrm{d}\Omega_0. \end{aligned} \tag{B7}$$

Thus, even in the case that the light source has a finite size, the SVA of the radiometer can be obtained in the same manner as in the case of the parallel light source.

Appendix C

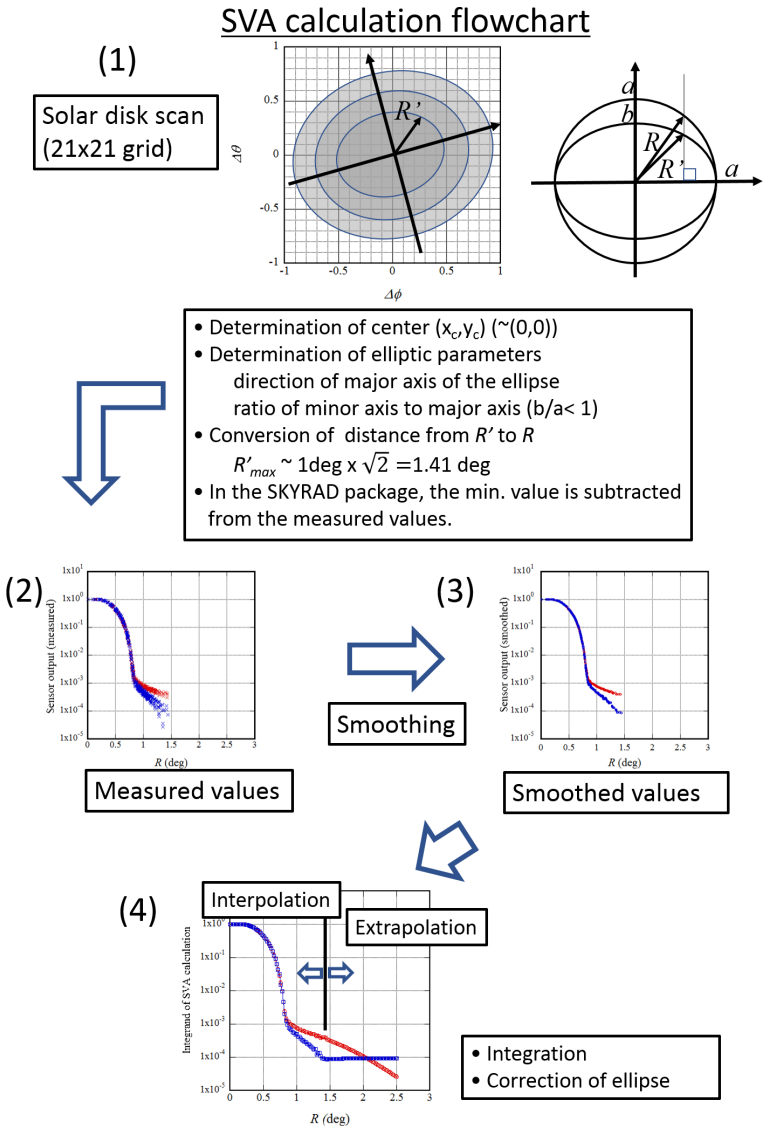

Figure C1. Flowchart of the SVA calculation procedure in the SKYRAD package.

Author contributions. This study was designed by AU and TM. The measurements of sky radiometer were conducted by AU and AK. Simulations and the analyses were performed by AU. The manuscript was written by AU, and all authors contributed to editing and revision.

Competing interests. The authors declare that they have no conflict of interest.

Special issue statement. This article is part of the special issue "SKYNET – the international network for aerosol, clouds, and solar radiation studies and their applications (AMT/ACP inter-journal SI)". It is not associated with a conference.

Acknowledgements. This work was supported by the NIES GOSAT-2 project, Japan. This work was also partially supported by JSPS KAKENHI grant number JP17K00531.

Edited by: Omar Torres
Reviewed by: one anonymous referee

References

Hashimoto, M., Nakajima, T., Dubovik, O., Campanelli, M., Che, H., Khatri, P., Takamura, T., and Pandithurai, G.: Development of a new data-processing method for SKYNET sky radiometer observations, Atmos. Meas. Tech., 5, 2723–2737, https://doi.org/10.5194/amt-5-2723-2012, 2012.

Hess, M., Koepke, P., and Schult, I.: Optical Properties of Aerosols and Clouds: The Software Package OPAC, B. Am. Meteorol. Soc., 79, 831–844, 1998.

Holben, B. N., Eck, T. F., Slutsker, I., Tanré, D., Buis, J. P., Setzer, A., Vermote, E., Reagan, J. A., Kaufman, Y. J., Nakajima, T., Lavenu, F., Jankowiak, I., and Smirnov, A.: AERONET-A federated instrument network and data archive for aerosol characterization, Remote Sens. Environ., 66, 1–16, 1998.

Khatri, P., Takamura, T., Nakajima, T., Estellés, V., Irie, H., Kuze, H., Campanelli, M., Sinyuk, A., Lee, S.-M., Sohn, B. J., Pandithurai, G., Kim, S.-W., Yoon, S. C., Martinez-Lozano, J. A., Hashimoto, M., Devara, P. C. S., and Manago, N.: Factors for inconsistent aerosol single scattering albedo between SKYNET and AERONET, J. Geophys. Res.-Atmos., 121, 1859–1877, https://doi.org/10.1002/2015JD023976, 2016.

Lohmann, U. and Feichter, J.: Global indirect aerosol effects: a review, Atmos. Chem. Phys., 5, 715–737, https://doi.org/10.5194/acp-5-715-2005, 2005.

Manago, N., Pradeep, K., Irie, H., Takamura, T., and Kuze, H.: On the method of solid view angle calibration for SKYNET skyradiometers, 4th International SKYNET workshop, Rome, Italy, 2–4 March, 2016.

Nakajima, T., Tonna, G., Rao, R., Kaufman, Y., and Holben, B.: Use of sky brightness measurements from ground for remote sensing of particulate polydispersions, Appl. Opt., 35, 2672–2686, 1996.

Ramanathan, V., Crutzen, P. J., Kiehl, J. T., and Rosenfeld, D.: Aerosols, Climate, and the Hydrological Cycle, Science, 294, 2119–2124, 2001.

Sinyuk, A., Holben, B. N., Smirnov, A., Eck, T. F., Slutsker, I., Schafer, J. S., Giles, D. M., and Sorokin, M.: Assessment of error in aerosol optical depth measured by AERONET due to aerosol forward scattering, Geophys. Res. Lett., 39, L23806, https://doi.org/10.1029/2012GL053894, 2012.

Takamura, T., Nakajima, T., and SKYNET community group: Overview of SKYNET and its Activities. Proceedings of AERONET workshop, El Arenosillo, Opt. Pura Aplicada, 37, 3303–3308, 2004.

Torres, B., Toledano, C., Berjón, A., Fuertes, D., Molina, V., Gonzalez, R., Canini, M., Cachorro, V. E., Goloub, P., Podvin, T., Blarel, L., Dubovik, O., Bennouna, Y., and de Frutos, A. M.: Measurements on pointing error and field of view of Cimel-318 Sun photometers in the scope of AERONET, Atmos. Meas. Tech., 6, 2207–2220, https://doi.org/10.5194/amt-6-2207-2013, 2013.

Uchiyama, A., Matsunaga, T., and Yamazaki, A.: The instrument constant of sky radiometers (POM-02) – Part 1: Calibration constant, Atmos. Meas. Tech., 11, 5363–5388, https://doi.org/10.5194/amt-11-5363-2018, 2018.

Zhao, F., Tan, Y., Li, Z., and Gai, C.: The effect and correction of aerosol forward scattering on retrieval of aerosol optical depth from Sun photometer measurements, Geophys. Res. Lett., 39, L14805, https://doi.org/10.1029/2012GL052135, 2012.